Structure of the Dysprosium–Glycocholate Complex in Submicellar Aqueous Solution: Paramagnetic Mapping by Proton Nuclear Magnetic Resonance Spectroscopy. An Approximation for the Intrinsic "Bound" Relaxation Rates in the Case of Nondilute Paramagnetic Systems†

Elizabeth Mukidjam,‡ Gabriel A. Elgavish,*,§,∥ and Stephen Barnes‡,∥

Departments of Biochemistry and Pharmacology and Division of Cardiovascular Disease, Department of Medicine, The Comprehensive Cancer Center and Cystic Fibrosis Research Center, University of Alabama at Birmingham, Birmingham, Alabama 35294

Received February 23, 1987; Revised Manuscript Received June 3, 1987

ABSTRACT: A paramagnetic NMR study of the structure of the calcium–glycocholate complex in submicellar solution, utilizing dysprosium as an isomorphous lanthanide replacement of calcium, is presented. The dysprosium-induced relaxation rate ($1/T_1$) enhancements of certain glycocholate protons have been used to estimate internuclear distances between these protons and the metal ion. An approximation to calculate the intrinsic relaxation rate ($1/T_1$) enhancements for a nondilute paramagnetic solution is given in the Appendix. From these data, and analysis based on conformation averaging and minimum energy conformations, a molecular model of the dysprosium–glycocholate complex in submicellar aqueous solution has been constructed. In this model the metal ion has a unidentate, first-sphere interaction with the proximal oxygen atom of the glycine carboxyl. The metal ion has second-sphere interactions with the peptide bond carbonyl oxygen (3.6 Å) and the distal carboxyl oxygen (4.4 Å). The metal ion to hydroxyl oxygen distances (8.4–12.4 Å) are not compatible with any metal ion to hydroxyl coordination. The side chain appears to exist in one predominant conformation. All six oxygen atoms of glycocholate, the peptide bond carbonyl, the carboxyl group, and the hydroxyl groups are on the α face of the bile salt molecule. On the basis of these features we conclude that in the submicellar state the solution structure of the dysprosium–glycocholate complex displays a metal ion enhanced segregation of polar versus nonpolar groups to the two separate faces of the molecule, which may result in a facilitated hydrophobic interaction of different complex units.

Bile salts are 24-carbon 5β-cholanoates, and conjugated to glycine (e.g., glycocholate, GC)[1] or taurine, they are the principal solutes in the bile. Bile salts have detergent-like, amphiphilic properties, and in aqueous solution, above their critical micellar concentration[2] (cmc), they undergo self-association to form micellar complexes that are in equilibrium with a smaller proportion of bile salt monomers (Small, 1971). At concentrations lower than the cmc, bile salts are assumed to exist as monomers.

Investigation of the physical chemistry of bile salts has attracted much attention since it has provided insights into the cause of cholesterol gallstone formation (Carey & Small, 1978). Several parameters that may govern the formation of cholesterol gallstones have been suggested. One of these, the presence in bile of polyvalent cations such as calcium, is thought to govern the rate of nucleation of bile supersaturated with cholesterol by promoting the fusion of phospholipid–cholesterol vesicles (Kibe et al., 1985). Since calcium is present in bile at concentrations exceeding the solubility product for several ionic species, it would be also expected to precipitate from the bile. That it does not do so suggests that Ca^{2+} ions are normally associated with other water-soluble complexes, of which the most likely are bile salts.

Several investigators (Williamson & Percy-Robb, 1979, 1980; Rajagopalan & Lindenbaum, 1982; Moore et al., 1982; Kahn et al., 1982; Moore, 1984; Marteau et al., 1985) have used Ca^{2+}-specific electrodes to show that a significant fraction of calcium in the bile is bound to bile salts. Recently, in this laboratory we have determined the stoichiometry and affinity of the Ca–GC complex by the analysis of paramagnetic lanthanide-induced changes in the chemical shifts of ^{1}H NMR resonances (Mukidjam et al., 1986). With this technique a 1:1 stoichiometry has been obtained for the Dy–GC complex with a dissociation constant of 4.15 mM. Further, in competition experiments with Ca^{2+}, the dissociation constant for the Ca–GC complex has been shown to be 9.5 mM, similar to the value found by the Ca^{2+}-specific electrode studies (9.6 mM; Moore, 1984), indicating that in a solution of 1 mM $CaCl_2$ and 1 mM glycocholate in equilibrium 9% of Ca^{2+} is present as Ca–GC complex.

† This study was supported in part by a grant from The Cystic Fibrosis Foundation and by funds from Grant AM-25511 from the National Institute of Arthritis, Digestive and Kidney Diseases. The NMR instrumentation used was supported in part by NIH Grant CA-13148 to the NMR Core Facility of the UAB Comprehensive Cancer Center. This work was presented in part at the Annual Meeting of The American Association for the Study of Liver Diseases, Chicago, IL, Nov 6–7, 1983 (Elgavish & Barnes, 1983).

* Address correspondence to this author at the Division of Cardiovascular Disease, Department of Medicine, University of Alabama at Birmingham, THT-327, Birmingham, AL 35294.

‡ Department of Pharmacology.

§ Division of Cardiovascular Disease, Department of Medicine.

∥ Department of Biochemistry.

[1] Abbreviations: GC, (3α,7α,12α-trihydroxy-5β-cholan-24-oyl)glycine (glycocholate); NMR, nuclear magnetic resonance; Gly, glycine; cmc, critical micellar concentration; EDTA, ethylenediaminetetraacetic acid; rf, radio frequency.

[2] Bile salts, unlike detergents such as sodium dodecyl sulfate, do not associate to form large micelles over a narrow concentration range. Although some investigators have introduced the terms uncritical multimer concentration or noncritical micellar concentration, rather than critical micellar concentration (cmc), we have chosen to use the more familiar term cmc.

0006-2960/87/0426-6785$01.50/0

The lanthanide ions, 4f transition metals with largely non-transition-metal-like chemistry, are considered as isomorphous replacements for calcium (Lee & Sykes, 1980; Sowadski et al., 1978; Horrocks & Sudnick, 1979; Darnall & Birnbaum, 1970; Matthews & Weaver, 1974; Reuben, 1979). Unlike calcium, however, they display a range of useful spectroscopical properties.

By use of lanthanide NMR shift and relaxation reagents, which range from the aquoions to various lanthanide complexes, the solution structure of small molecules (Reuben & Elgavish, 1979) and of the metal ion binding pocket of macromolecules (Reuben, 1979) can be mapped.

The effect of the paramagnetic lanthanide Dy^{3+} on the spin–lattice relaxation rate ($1/T_1$) can be used to deduce the distances between the metal ion and various atoms in the ligand. Proton relaxation rate data, therefore, yield the average distances between the Dy^{3+} ion and the bile salt protons and hence can be utilized to build a structural model of the Dy–GC complex.

In this study we have used paramagnetic lanthanide NMR mapping to determine the solution structure of the Dy–GC complex in dilute nonmicellar, aqueous solution. Since the side chain is considered to be a factor in the assembly of micelles (Roda et al., 1983; Hogan et al., 1984), the structure of the side chain in the nonmicellar complexes is of particular importance. From the data obtained in this study it is postulated that the side chain of the metal complex is held in a particular conformation, rather than being allowed to rotate freely. This implies that micelle formation by glycocholate would be facilitated by complexation with Ca^{2+}.

Experimental Procedures

Analytical-grade chemicals were used throughout. Sodium glycocholate (Sigma Chemical Co., St. Louis, MO) was extracted at pH 5 with ethyl acetate to remove cholic acid. The solution was acidified with HCl and the precipitated glycocholic acid extracted with diethyl ether. After removal of solvent, the glycocholic acid was dissolved in a minimum volume of ethanol and titrated to pH 7 with aqueous NaOH and then freeze-dried. The amorphous sodium salt was dissolved in deuterium oxide (Aldrich Chemical Co., Milwaukee, WI; 99.8% D). The pH was adjusted to 9 and the sample lyophilized to remove residual H_2O. The glycocholate solutions were freshly prepared from this material. Bile salt concentrations were determined by a 3α-hydroxysteroid dehydrogenase procedure (Barnes & Spenney, 1980).

Dysprosium (99.998%) and lanthanum (99.999%) chlorides were purchased from Aldrich. Stock solutions were prepared in deuterium oxide, dried under vacuum in a Rotavapor over a 50 °C water bath, and redissolved in D_2O. Lanthanide concentrations were determined by EDTA titration in the presence of pyridine as buffer, and arsenazo was used as end-point indicator.

^1H NMR spectra of the bile salt complexes were obtained at 400 MHz on a Bruker WH-400 spectrometer of the NMR Core Facility of the UAB Comprehensive Cancer Center. Samples of about 0.5-mL volume were contained in 5 mm o.d. NMR tubes. A pulse repetition time of 2 s, spectral width of 4000 Hz, 16K memory, and line broadening of 1 Hz were employed. The T_1 measurements were done by the inversion recovery method with a π–τ–$\pi/2$ pulse sequence automatically controlled by the spectrometer processor.

Rhodamine absorbance was measured at λ = 545 and 515 nm on an LKB UV/vis Ultraspec spectrophotometer. Samples were prepared containing 1 μM rhodamine and various concentrations of sodium glycocholate titrated to pH 5. To these control solutions was added 150 mM NaCl or 50 mM $CaCl_2$ and the absorbances were measured.

Methods of Data Analysis. The observed relaxation rate $1/T_1$ for a nucleus in a ligand exchanging between free bulk and metal ion bound states is given by (Leigh, 1971)

$$1/T_1 = 1/T_{1F} + N_M/N_F(\tau_M + T_{1M}) \quad (1)$$

This equation is an approximation which is valid in systems of dilute solutions of paramagnetic spins, where the following conditions prevail:

$$T_{1F} \gg T_{1M} \text{ and } \tau_F \gg \tau_M$$

where τ_F and τ_M are the lifetimes of the species in the magnetic environment (F) as free ligand and (M) bound to paramagnetic cation, respectively. N_M/N_F is the ratio of the number of nuclei in the metal ion bound species relative to the free, unbound species, and $1/T_{1F}$ and $1/T_{1M}$ are the relaxation rates of the free ligand and the metal ion bound ligand, respectively.

In many systems of weak lanthanide complexes, the above condition of dilute species does not apply in most experimental circumstances. Nevertheless, we have shown (see Appendix) that eq 1 can be also obtained by use of assumptions that are appropriate for systems of weak lanthanide complexes and similar systems. In the case of Dy–GC, one can easily show that since δ_M(Gly-α) = 28 ppm (Mukidjam et al., 1986) and conditions of fast exchange do prevail, the lower limit for τ_M is of the order of 10^{-5} s. With $\tau_M \ll T_{1M}$, eq 1 becomes

$$1/T_1 = 1/T_{1F} + (N_M/N_F)(1/T_{1M}) \quad (2)$$

where $1/T_1$ is the observed relaxation rate, $1/T_{1F}$ is the relaxation rate in the free diamagnetic state, and $1/T_{1M}$ is the intrinsic relaxation rate in the bound state. The concentrations of the bound ligand, ML, may be readily calculated from the total concentrations of ligand and metal ion by use of the dissociation constant obtained from the chemical shift data (Mukidjam et al., 1986). The concentration of the free ligand is calculated by subtracting the bound concentration from the total ligand concentration. The observed $1/T_1$ induced by a diamagnetic lanthanide, lanthanum (La^{3+}), under experimental conditions similar to the dysprosium system is given by

$$1/T_1(La^{3+}) = 1/T_{1F} + (N_M/N_F)(1/T_{1\infty}) \quad (3)$$

where $1/T_{1\infty}$ stands for the diamagnetic coordination-induced relaxation rate contribution.

When $1/T_1(La^{3+})$ data are subtracted from the $1/T_1(Dy^{3+})$ data, the net paramagnetic effect ($1/T_{1p}$) is obtained:

$$1/T_{1p} = (N_M/N_F)(1/T_{1M}') \quad (4)$$

where $1/T_{1M}'$ is the intrinsic, net paramagnetic relaxation rate.

These intrinsic, lanthanide-induced, paramagnetic, longitudinal relaxation rates are of dipolar origin. For dysprosium, for a given nucleus i, it is a sum of two contributions, the Solomon term $1/T_{1MS}(i)$ (Solomon, 1955) and the susceptibility term $1/T_{1MX}(i)$ (Gueron, 1975; Vega & Fiat, 1976):

$$1/T_{1M}'(i) = 1/T_{1MS}(i) + 1/T_{1MX}(i) \quad (5)$$

Their dependence on the metal ion–proton distance (for lanthanides except Gd) is described by

$$1/T_{1MS}(i) = Cr^{-6}(i)f(T_{1e},\omega_I,\omega_S) \quad (6)$$

with

$$f(T_{1e},\omega_I,\omega_S) = 3T_{1e}/(1 + \omega_I^2T_{1e}^2) + 7T_{1e}/(1 + \omega_S^2T_{1e}^2)$$

and

$$1/T_{1MX}(i) = BH_o^2r^{-6}(i)f(\tau_r,\omega_I) \quad (7)$$

with

$$f(\tau_r,\omega_I) = \tau_r/(1 + \omega_I^2\tau_r^2)$$

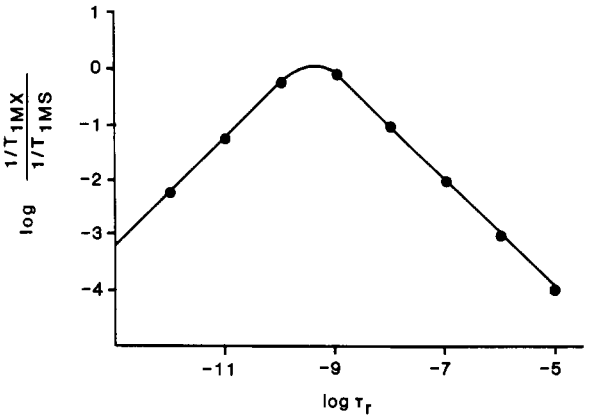

FIGURE 1: Dependency of the susceptibility contribution of the relaxation rate on the rotational correlation time calculated for an external magnetic field of 9.4 T. log $(T_{1MX}^{-1}/T_{1MS}^{-1})$ is plotted vs log τ_r.

where B and C are magnetic constants characteristic of the observed nucleus and the lanthanide employed, H_0 is the external magnetic field, T_{1e} is the electronic relaxation time of the lanthanide, τ_r is the molecular tumbling time, proportional to the size of the complex, ω_I and ω_S are the Larmor frequencies, at the given external magnetic field, of proton and electron, respectively, and $r(i)$ are the nucleus to metal ion distances of nuclei i. The relative importance of these two terms can be determined by dividing eq 7 by eq 6 to give (Lenkinski, 1984)

$$T_{1MX}^{-1}/T_{1MS}^{-1} = (B/C)H_0^2[\tau_r/(1 + \omega^2\tau_r^2)]T_{1e}^{-1} \quad (8)$$

and is shown in Figure 1 as a plot of log $(T_{1MX}^{-1}/T_{1MS}^{-1})$ vs log τ_r, calculated for H_0 = 94 kG and $T_{1e} = 0.78 \times 10^{-12}$ s (Burns & LaMar, 1982). Under these conditions, the ratio $T_{1MX}^{-1}/T_{1MS}^{-1}$ has the largest effect for molecules with τ_r between 10^{-10} and 10^{-9} s. Therefore, in such systems, the susceptibility contribution has to be taken into consideration for the calculation of distances between the paramagnetic ion and the nuclei. For smaller molecules, with $\tau_r \sim 10^{-11}$ s, and larger molecules, with $\tau_r \sim 10^{-8}$ s, the ratio $T_{1MX}^{-1}/T_{1MS}^{-1}$ is small, so that the contribution of T_{1MX}^{-1} to the intrinsic relaxation rates $1/T_{1M}'$ in eq 5 tends to be negligible.

With use of the observed relaxation rates, the intrinsic paramagnetic relaxation rates are calculated from eq 4. The distance r of each nucleus from the paramagnetic metal ion is then calculated from eq 5–7, with

$$B = (6/5)\frac{\gamma^2 g^4 \beta^4 J^2(J + 1)^2}{(3kT)^2}$$

and

$$C = (2/15)\gamma^2 g^2 \beta^2 J(J + 1)$$

The characteristic magnetic constants used for the proton and dysprosium are $\gamma_{(H)} = 2.68 \times 10^4$ rad G^{-1} s^{-1}, $g_{(Dy)} = 4/3$, $\beta = 9.274 \times 10^{-21}$ erg G^{-1}, and $J_{(Dy)} = 15/2$. The other constants used are $k = 1.38 \times 10^{-16}$ erg K^{-1} and T = 300 K. The Larmor frequency for a proton at H_0 = 94 kG is $\omega_I = 2.51 \times 10^9$ s^{-1} and for an electron is $\omega_S = 1.65 \times 10^{12}$ s^{-1}.

The correlation time for Dy–GC is calculated from

$$\tau_r = \frac{4\Pi\eta a^3}{3kT}$$

with η = viscosity and a = mean radius of the molecule. With the H_2O molecule as a reference with a (H_2O) = 1.58 Å and

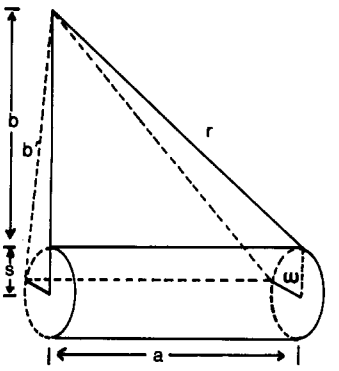

FIGURE 2: A model to calculate the conformational averaging of the distance from a methyl group to the metal ion.

$\tau_r(H_2O) = 2.7 \times 10^{-12}$ (Poole, 1971), the correlation time for a Dy–GC molecule with a mean radius of a = 5.8 Å is calculated as $\tau_r = 1.3 \times 10^{-10}$ s.

The distance of each nucleus from the Dy^{3+} is then calculated by use of this correlation time, and a molecular model is then constructed. Refinements of the position of the three methyl groups is done by carrying out conformational averaging following the method of Lenkinski and Reuben (1976). The model used for this calculation is shown in Figure 2. The distance in space from the lanthanide X to the rotating circle with a radius s of the methyl group is $r(\omega)$. The distance b is obtained if the point X is projected to the extension of the rotating axis of the methyl group and a is the length of the extended axis of the methyl group to the projected point X′. After rotation through ω radians, $r^2(\omega)$ is given by

$$r^2(\omega) = a^2 + (b + s)^2 + s^2 - 2s(b + s)\cos\omega \quad (9)$$

When free rotation exists, the average value of $1/r^6$ is applicable, and $[1/r^6]_{av}$ is given by

$$[1/r^6]_{av} = (1/2\Pi)\int d\omega/(r^2(\omega))^3 \quad (10)$$

The integral in eq 10 is evaluated for the methyl groups according to the trapezoidal rule, and the distances obtained from the relaxation rate data are corrected accordingly (see Table I).

A further question is to determine whether the side chain is able to rotate freely or it is in a particular configuration. To answer this, the average position of the Dy^{3+} ion, in rectangular coordinates, is estimated with its distances (r_i) (Table I) from the protons on the steroid ring (i.e., 3β, 7β, 12β, 18-CH_3, 19-CH_3, and 21-CH_3). The following equation is solved by the program NLIN[3] with the weighting term $1/r_i^6$:

$$x^2 + y^2 + z^2 - 2(a_i x + b_i y + c_i z) + a_i^2 + b_i^2 + c_i^2 = r_i^2 \quad (11)$$

where x, y, and z are the coordinates of the Dy^{3+} ion and a_i, b_i, and c_i are the coordinates of the ith proton. The latter coordinates are derived from the previously published data for the crystal structure of calcium cholate chloride heptahydrate (Hogan et al., 1984) (Table II).

The side chain of glycocholate is illustrated in Figure 3. The definition of the angles ω, ϕ, ψ, and χ correspond to the angles used for the description of polypeptide conformers (IUPAC–IUB, 1969). The torsion angles are defined for each successive pair of atoms in the side chain as shown in the inset in Figure 3. Looking directly at the bond between the front

[3] The NLIN program is part of the SAS package, SAS Inc., Cary, NC, 1980.

Table I

proton	$1/T_1$ (s^{-1})[a]	$1/T_{1p}$ (s^{-1})[b]	$1/T_{1M}'$ (s^{-1})[c]	r (Å)[d]
3β	4.40 ± 40%	0.23 ± 47%	2.17 ± 47%	12.6 ± 1.1
7β	5.40 ± 28%	0.40 ± 32%	3.68 ± 32%	11.5 ± 0.6
12β	6.25 ± 12%	0.71 ± 13%	6.53 ± 13%	10.4 ± 0.2
18-CH_3	3.40 ± 4%	0.56 ± 5%	5.15 ± 5%	10.6[e] ± 0.1
19-CH_3	3.00 ± 5%	0.14 ± 5%	1.29 ± 5%	13.3[e] ± 0.1
21-CH_3	6.00 ± 4%	2.77 ± 4%	25.49 ± 4%	9.1[e] ± 0.1
23-CH_3	18.00 ± 3%	13.83 ± 4%	127.28 ± 4%	6.37 ± 0.03
Gly(α)-CH_2	92.00 ± 3%	90.00 ± 4%	828.32 ± 4%	4.65 ± 0.03

[a] Observed relaxation rates ± percent error. The error calculation is from NLIN fitting. [b] Paramagnetic contribution, calculated from the observed rates by correcting for the diamagnetic contributions ± percent error (see eq 3). The error calculation is the sum of the observed and the diamagnetic contribution of the relaxation rates. [c] Intrinsic paramagnetic relaxation rate ± percent error, calculated from eq 4. [d] Internuclear distances calculated from the intrinsic relaxation rates with eq 5–7. [e] Corrected internuclear distances, calculated using conformational averaging (see eq 10).

Table II: Atom Positions on Semirigid Steroid Rings of Calcium Cholate[a]

name	X	Y	Z
C_3	17.639	2.791	4.570
O_3	18.316	2.915	3.320
$H_{3\beta}$	18.346	3.058	5.342
C_7	13.194	3.798	5.283
O_7	13.426	4.008	3.869
$H_{7\beta}$	12.614	2.433	6.600
C_{12}	12.701	−0.552	4.819
O_{12}	13.044	−0.514	3.424
$H_{12\beta}$	12.521	−1.485	4.995
C_{18}	11.064	0.104	6.632
H_{18}	10.949	−0.759	6.904
H_{18}	11.709	0.514	7.314
H_{18}	10.123	0.572	6.840
C_{19}	14.996	1.882	7.839
H_{19}	14.707	0.857	8.300
H_{19}	15.628	2.237	8.379
H_{19}	14.181	2.414	8.105
C_{21}	10.012	−2.477	4.623
H_{21}	9.537	−3.148	4.798
H_{21}	10.561	−2.643	3.878
H_{21}	10.595	−2.424	5.443

[a] The positions of atoms that were used to determine the side-chain structure of the Dy–GC complex were obtained from the X-ray crystal structure of calcium cholate heptahydrate [Hogan et al. (1984), Table II] and are converted to the Cartesian coordinate system.

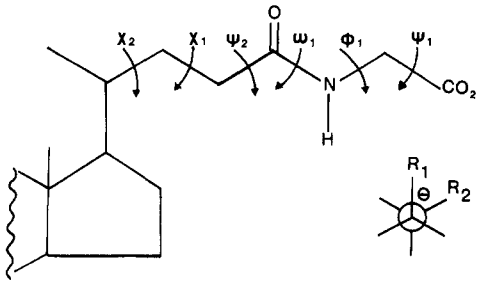

FIGURE 3: Definitions of ϕ, ψ, ω, and χ dihedral angles in the side chain of the glycocholate molecule. (Inset) Standard convention to define the torsion angles θ, using four atoms in sequence order along the side chain. O is the front C atom; • is the rear C atom; R_1 is the front bond and used as reference; R_2 is the rear bond. θ is the angle between R_1 and R_2.

atom and the preceeding atom in the side chain as a stationary reference to define 0°, the torsion angle is positive if the direction of the bond between the rear atom and the rest of the side chain is clockwise from 0° and negative if it is counterclockwise.

To determine the conformation of the side chain in the Dy–GC complex, two assumptions have been made: the C_{21} methyl group is placed in the same position as in the crystal structure of calcium cholate and the torsion angle of the peptide bond ω_1 is set to 180°, reflecting a trans planar configuration. Consideration of motion in the side chain has been

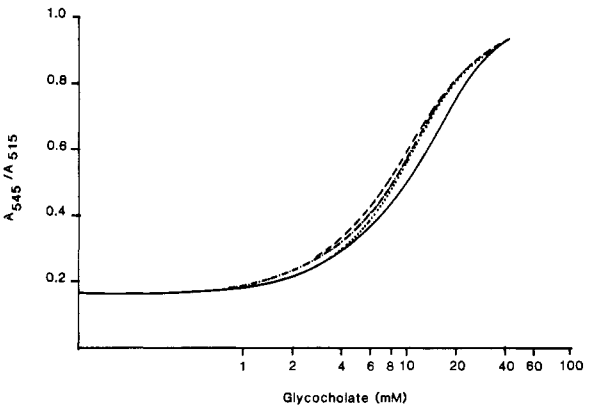

FIGURE 4: Effect of metal ions on the shift in rhodamine absorbance. The solid line is the rhodamine absorbance vs glycocholate concentration. Rhodamine absorbance (−·−) after addition of 10 mM $CaCl_2$, (−−) after addition of 50 mM $CaCl_2$, and (···) after addition of 150 mM NaCl.

carried out by two alternative methods: first, free rotation (i.e., all possible conformers) about each bond and, second, examination of the minimum energy conformations. The former type of analysis has been performed on an Apple IIe computer, and the latter analysis has been carried out with an Evans and Sutherland computer graphics system supported by a VAX 1180 computer. The three-dimensional on-line graphics capability enables the positioning of the side chain, as it rotates about each of the bonds, to conform to the minimum energy requirements. In this way, the distance from the Dy^{3+} ion to the protons for each conformation can be calculated by the computer and compared to the experimentally determined value. This procedure has enabled the selection of the conformation that best fits the observed data.

RESULTS

Spectroscopic Evaluation of cmc. The rhodamine absorbance ratio is shown as a function of glycocholate concentration in Figure 4. The rhodamine absorbance ratio A_{545}/A_{515} at glycocholate concentrations less than 4 mM is much lower than at glycocholate concentrations above the cmc (greater than 4 mM). The steeper slopes obtained upon the addition of 150 mM NaCl or 50 mM $CaCl_2$ indicate that at the same concentration of GC more micelles are formed in the presence of the metal ions. However, at GC concentrations lower than 2 mM, the absorbance ratio of rhodamine, A_{545}/A_{515}, does not change significantly, indicating that GC in this concentration range is present primarily as monomer, irrespective of whether $CaCl_2$ or NaCl is present.

NMR Experiments. The ^1H NMR spectrum of 0.5 mM sodium glycocholate in D_2O, at pH 5, is depicted in Figure 5. There are at least 10 well-resolved resonances: the single protons geminal to each of the three hydroxyls, i.e., 3β, 7β,

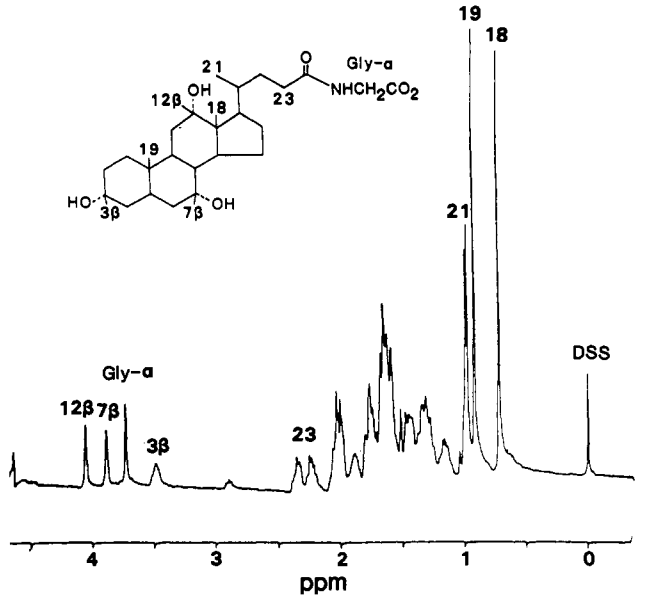

FIGURE 5: The 400-MHz ^1H NMR spectrum of 0.5 mM glycocholate in D_2O, pH 5, at 21 °C.

and 12β; the three methyl groups 18, 19, and 21; one proton from the ring methylene 16; the side-chain methylenes 23 (A and B protons) and the glycine α-methylene protons, Gly(α).

Identification of the various resonances has been done according to the previously published assignments (Barnes & Geckle, 1982). The distances of protons on the glycocholate molecule to the Dy^{3+} ion have been calculated from eq 3–7. The distances to the methyl groups have been corrected by conformational averaging (see Experimental Procedures). The observed, the net paramagnetic, and the intrinsic paramagnetic longitudinal relaxation rates for eight protons in the Dy–GC complex, and their distances from the Dy^{3+} ion, are compiled in Table I. The strong dependence of $1/T_{1M}'$ on the internuclear distance is clearly manifest through an almost 3 orders of magnitude variation between the intrinsic relaxation rates of the proton resonances of the Gly(α) and methyl 19, whereas the ratio of their distances is less than 3. This amplification makes the determination of distances, based on dipolar relaxation rate enhancements, accurate to better than 0.1 Å for most nuclei.

Determination of Structure of the Dy^{3+}–GC Complex. The positions of the hydrogen atoms on the semirigid steroid nucleus, as obtained from the crystal structure, are used to determine the position of the Dy^{3+} ion in the same rectangular coordinate system and are compiled in Table II [from Hogan et al. (1984)]. By use of these positions in space and the distances of the Dy^{3+} to the protons 3β, 7β, 12β, 18-CH_3, and 19-CH_3 obtained from the NMR data, the position of the Dy^{3+} ion was found by nonlinear regression analysis to be 8.56, −0.22, −3.72 in rectangular coordinates, with an accuracy better than ±0.5 Å (see Experimental Procedures, eq 11).

Table III: Atom Positions on the Side Chain of the Dy–GC Complex

name	X	Y	Z
C_{22}	8.291	−1.189	3.258
H_{22}	7.726	−0.324	3.386
H_{22}	7.649	−1.901	3.280
C_{23}	9.028	−1.375	1.959
H_{23}	9.561	−2.110	2.343
H_{23}	9.441	−0.622	1.886
C_{24}	8.125	−1.417	0.751
O_{24}	8.624	−1.618	−0.380
N	6.801	−1.300	0.913
H(N)	6.365	−1.164	1.803
C(α)	5.848	−1.335	−0.228
H(α)	5.999	−2.102	−0.767
H(α)	4.958	−1.392	−0.101
$C(CO_2^-)$	6.078	−0.097	−1.110
O_A	5.367	0.901	−0.853
O_B	6.946	−0.168	−1.995
Dy^{3+}	8.560	−0.220	−3.720

Free rotation of the side chain about the C_{20}–C_{22} bond has led to a calculated averaged distance of 5.47 and 5.27 Å from the newly positioned Dy^{3+} ion to the two H_{23} protons, considerably shorter than the experimentally observed distance (6.37 Å) (Table I). Consideration of the three minimum-energy conformers about the C_{20}–C_{22} bond has shown that only one yields a metal ion–proton (H_{23}) distance close to the observed distance. Of the other two conformers, one would have also had steric hindrance from the D-ring protons. This has enabled selection of values of 61° and 180° for the angles χ_2 and χ_1, respectively (Figure 3).

The amide bond has been assumed to be planar, with the carbonyl at 180° to the NH group. Therefore, the position of $C_{Gly(\alpha)}$ depends on the rotation of the C_{23}–C_{24} bond. Since the H_{22}–N(H) distances are ~2 Å, the plane of the amide bond is placed so that the nitrogen-bound proton is staggered with respect to the H_{22} protons. For a similar reason, the N–$C_{Gly(\alpha)}$ bond is rotated so that the Gly(α) protons are staggered with respect to the nitrogen-bound proton. The distance from the Dy^{3+} to the Gly(α) protons in this model is close to the observed value, whereas the average distance, obtained by assuming free rotation, does not match the observed value. Finally, the rotation of the carboxyl group around the $C_{Gly(\alpha)}$–$C_{Gly(CO_2^-)}$ bond has been considered. A bidentate interaction between the metal ion and both of the carboxyl oxygen atoms is possible; however, one of the carboxyl oxygens is then found ~2 Å from the carbonyl oxygen atom. It has been, therefore, necessary to propose a unidentate metal ion to carboxyl interaction to yield the conformer with the lowest energy. With this conformer a three-dimensional structure has been constructed, and is shown as a computer-drawn stereo picture in Figure 6, with $\chi_2 = 61°$, $\chi_1 = 180°$, $\psi_2 = 0°$, $\omega_1 = 180°$, $\phi_1 = -66°$, and $\psi_1 = -93°$. ψ_1 is the angle between N–$C_{Gly(\alpha)}$ and C–O distal. The positions of the atoms on the side chain of the glycocholate and the Dy^{3+} ion are compiled in Table III.

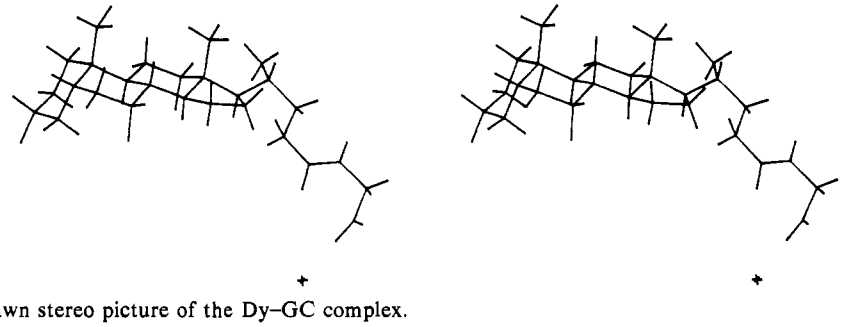

FIGURE 6: Computer-drawn stereo picture of the Dy–GC complex.

Discussion

On the basis of the dysprosium–proton distances obtained for eight sets of protons, distributed among the different parts of the metal ion bound glycocholate molecule, we have been able to construct a model (Figure 6) of the Dy–GC complex in solution at a submicellar concentration. Of considerable importance, the data show that the GC side chain, instead of undergoing free rotation, must display quite restricted motion. In the conformation that is consistent with the observed data, the side chain extends away from the steroid rings and lies approximately in the plane of the B, C, and D rings, except for the carboxyl which is turned around by about 90° and is parallel to the A ring. The peptide bond carbonyl, the carboxyl group, and the hydroxyl groups are all on the α face of the bile salt molecule. This orientation would allow for greater possibility of intermolecular association as the GC concentration rises toward the cmc and predicts that the cmc will be lowered by the presence of the metal ion. We have indeed observed (Figure 4) that over the concentration range of 4–15 mM the fraction of glycocholate micelles/monomers is greater in the presence of metal ions.

As we have previously suggested from analysis of chemical shift data (Mukidjam et al., 1986), the data in the present study show that the metal ion is located close to the carboxylate group, away from the steroid rings. The position of the metal ion has been determined from distances of protons attached to the semirigid steroid nucleus. The positions of these protons were obtained from crystal structure data (Hogan et al., 1984). However, the side-chain conformation cannot be determined directly since it is possible that each of the distances from the metal ion to observable side-chain protons is a weighted average of several conformers. In any case, there is the usual risk that crystal structure data of a mobile side chain are governed by forces different from those which operate in solution.

From inspection of the possible side-chain orientation obtained by conformational analysis, the conformer with the lowest energy indicates that there is a monodentate interaction of the carboxyl group with the dysprosium. Attempts to rotate the carboxyl group such that the metal ion be on the bisector of the carboxyl group, and hence have bidentate interaction, would result in an unreasonably close proximity between one of the carboxyl oxygens and the peptide carbonyl oxygen. In Ca^{2+}–carboxylate complexes, monodentate interaction has been observed when the coordination number of Ca^{2+} is 6. At higher coordination numbers both mono- and bidentate interactions are possible (Einspahr & Bugg, 1981). In crystals of calcium cholate chloride heptahydrate, calcium has a bidentate interaction with the carboxylate group (Hogan et al., 1984). However, cholate does not have a peptide bond carbonyl that could interfere with the complexation of calcium with the carboxylate group. Future X-ray diffraction experiments on calcium–glycocholate crystals, albeit in the solid state, may clarify this issue. In our model the distance between the proximal oxygen of the carboxyl group and the dysprosium ion has been shown to be 2.4 Å. This distance is consistent with a first-sphere interaction. The 3.6-Å distance between the metal ion and the carbonyl oxygen is consistent with a second-sphere interaction between them, as is the distance between the distal oxygen of the carboxyl group and the metal ion (4.4 Å). The metal ion to hydroxyl oxygen distances, calculated from the positions of the metal ion and those of the hydroxyl group (see Table II) (8.4–12.4 Å), on the other hand, are incompatible with any metal ion to hydroxyl coordination. This is contrary to previous suggestions (Moore, 1984; Moore et al., 1985) that the complexation of calcium to bile salts involves hydroxyl groups.

It is most likely that the Ca–GC solution structure is similar to the one we have determined for the Dy–GC complex, since the lanthanides have been shown in several systems to be isomorphous replacements for calcium (Lee & Sykes, 1980; Sowadski et al., 1978; Horrocks & Sudnick, 1979; Darnall & Birnbaum, 1970; Matthews & Weaver, 1974; Reuben, 1979). Also, calcium has been shown to compete for the same binding site on GC as dysprosium and has a dissociation constant of 9.5 mM (Mukidjam et al., 1986), slightly larger than the 4.15 mM for the Dy–GC complex.

Calcium concentrations in bile are in the millimolar range (Wheeler, 1968), close to the dissociation constant of the Ca–GC complex. Since monomeric glycocholate is always present in equilibrium with the micelles in bile, Ca^{2+} and other polyvalent metal ions binding to GC monomers should have a significant contribution to the total binding of Ca^{2+} and other polyvalent metal ions in bile.

Nonmicellar complexes of the type we have described in this study occur in bile in equilibrium with micellar complexes. The weaker affinity of the latter for calcium may result in a relatively small micellar contribution to calcium binding in bile (Moore et al., 1982). The formation of the monomeric nonmicellar complex may also be important in certain hepatic and gastrointestinal diseases, i.e., cholestasis, ileal disorders, tropical sprue, and cystic fibrosis. In these diseases intestinal, intraluminal concentrations of bile salts are often reduced (Westergaard, 1977; Bevan et al., 1974) to what is considered to be submicellar levels. On the other hand, the concentration of calcium, due to its partially dietary origin, remains relatively constant. Consequently, a significant fraction of the bile salts will form nonmicellar calcium complexes which could then nonetheless promote micelle formation in spite of the low bile salt concentration.

Acknowledgments

We thank Dr. Mike Carson, Dr. Steve Ealick, and Scott Rowland, X-ray Crystallography Group, Department of Biochemistry, UAB, for their assistance in the preparation of the stereo picture of the bile salt complex.

Appendix

(I) The modified Bloch equations for the magnetizations in the direction of the external magnetic field, including exchange terms (McConnell, 1958), and in the absence of rf, are

$$\begin{aligned} dM_{zA}/dt &= M_{oA}R_{1A} - M_{zA}k_{1A} + M_{zB}k_B \\ dM_{zB}/dt &= M_{oB}R_{1B} - M_{zB}k_{1B} + M_{zA}k_A \end{aligned} \quad \text{(A1)}$$

where A and B denote the two different chemical environments between which chemical exchange takes place (e.g., A is a free ligand and B is the metal-bound ligand), M_{oA} and M_{oB} denote the corresponding equilibrium magnetizations in the direction of the external magnetic field, M_{zA} and M_{zB} denote the corresponding magnetizations in the direction of the external magnetic field, R_{1A} and R_{1B} denote the intrinsic relaxation rates in the absence of exchange, and k_A and k_B denote the reciprocal lifetimes, such that

$$R_{1A} \equiv 1/T_{1A} \qquad k_A \equiv 1/\tau_A \qquad R_{1B} \equiv 1/T_{1B} \qquad k_B \equiv 1/\tau_B \quad \text{(A2)}$$

and

$$k_{1A} \equiv R_{1A} + k_A \qquad k_{1B} \equiv R_{1B} + k_B \quad \text{(A3)}$$

The exact value for the generalized relaxation rate $\bar{R}_1$ can be obtained from the above equations (Leigh, 1971) and expressed as

$$-\bar{R}_1 = -Q \pm [Q^2 + W]^{1/2} \quad \text{(A4)}$$

where

$$Q \equiv (1/2)(k_{1A} + k_{1B}) \qquad W \equiv -(k_{1A}k_{1B} - k_A k_B) \quad \text{(A4a)}$$

Leigh (1971) derived from the above an approximate expression for R_1 in the case of dilute solutions of paramagnetic species using the assumptions that the concentration of the nuclei bound to the paramagnetic center relative to the free, or unbound, nuclei was negligible and that the relaxation rate in the unbound state was much larger than in the free. The two assumptions amount to the inequalities

$$R_{1B} \gg R_{1A} \qquad k_B \gg k_A \quad \text{(A5)}$$

With these assumptions he obtained

$$1/\bar{T}_1 = 1/T_{1A} + N_B/N_A(\tau_B + 1/T_{1B}) \quad \text{(A6)}$$

where N_B/N_A was the ratio of the number of nuclei in the metal-bound species relative to the free, unbound species. The same expression had been previously obtained by other investigators (McConnell, 1958; O'Reilly & Poole, 1968; Luz & Meiboom, 1964; Bloembergen & Morgan, 1961).

(II) Complex formation of a metal ion M (e.g., a paramagnetic lanthanide) with a ligand L, assuming a 1:1 stoichiometry, is described by

$$\underset{\text{state A}}{M + L} \underset{k_d}{\overset{k_f}{\rightleftharpoons}} \underset{\text{state B}}{ML} \quad \text{(A7)}$$

where k_f and k_d are the kinetic rate constants of the formation and dissociation of the metal–ligand complex ML, respectively. The lifetimes of a nucleus on ligand L in states A and B are τ_A and τ_B, respectively. Let us define reciprocal lifetimes k_A and k_B such that

$$k_A \equiv 1/\tau_A \qquad k_B \equiv 1/\tau_B \quad \text{(A8)}$$

Assuming first-order kinetics for the dissociation of the complex

$$k_B = k_d \quad \text{(A9)}$$

Since the dissociation constant K_d can be expressed as

$$K_d = [M][L]/[ML] \text{ as well as } K_d = k_d/k_f \quad \text{(A10)}$$

and since

$$\tau_A/\tau_B = [L]/[ML] \quad \text{(A11)}$$

it is easily shown that

$$k_A = [M]k_f \quad \text{(A12)}$$

Desolvation of the metal ion generally has been considered as the rate-determining step in the formation of lanthanide complexes (Lenkinski, 1984; Nieboer, 1975; Purdie & Farrow, 1973a,b; Choppin, 1971). This, as well as experimental data on several ligand systems, has suggested that the rate constant of lanthanide complex formation depends very little on the particular ligand and that τ_f is 10^{-6}–10^{-7} M·s (Lenkinski, 1984).

For weak lanthanide complexes, due to limited solubility, aggregate formation (e.g., micelles), or other experimental or theoretical (Lenkinski et al., 1978) considerations, the concentrations of metal ion and ligand may be limited to the same order of magnitude as the dissociation constant (K_d). In such systems the concentration of free metal ion, [M], will also be of the same order as K_d. Consequently

$$k_A = [M]k_f \sim K_d k_f = (k_d/k_f)k_f = k_d = k_B \quad \text{(A13)}$$

indicating that both reciprocal lifetimes in the exchange process are of the same order of magnitude, and

$$k_B \sim k_A = [M]k_f \quad \text{(A14)}$$

Using the experimental range found for the value of τ_f (10^{-6}–10^{-7} M·s) and the typical range of 10^{-3}–10^{-2} M for K_d of weak lanthanide complexes, one obtains $k_B \sim k_A$ in the 10^3–10^5 s^{-1} range.

(III) The approximation of dilute paramagnetic species (see section I) quite frequently cannot be made. This is the case with most weak lanthanide (other than Gd) complexes. The following alternative derivation is possible:

$$k_{1A} \sim k_A$$

since R_{1A}, as a diamagnetic relaxation rate, is of the order of 1 for nonquadrupolar nuclei. Therefore, it can be shown that

$$W \sim -k_A R_{1B} \quad \text{(A15)}$$

One can also easily show that the term Q^2 (see eq A4a) can be approximated, using the exchange information outlined in section II, as

$$Q^2 \sim k_A^2 + k_A R_{1B} \quad \text{(A16)}$$

Typical values for the intrinsic relaxation rate, R_{1B}, for nuclei at distances of 5 Å and above from the metal ion, in complexes of lanthanides other than gadolinium, are of the order of 10^2–10^0 s^{-1} (see, e.g., Table I). Therefore, $|W|$ is in the range of 10^3–10^7, whereas the corresponding range for $|Q^2|$ is 10^6–10^{10}. Consequently

$$|W|/|Q^2| \sim 10^{-3} \ll 1 \quad \text{(A17)}$$

Therefore, when eq A4 is rewritten as

$$\bar{R}_1 \sim Q\{1 \pm [1 + W/Q^2]^{1/2}\} \quad \text{(A18)}$$

the expression under the square root can be then replaced by a power series developed in terms of x, where $x = W/Q^2$:

$$[1 + x]^{1/2} = 1 + (1/2)x - (1/8)x^2 + (1/16)x^3 - \ldots \quad \text{(A19)}$$

Consequently, using eq 18 and 19, the observed relaxation rate, when only the first two terms of the power series are used, is given by

$$\bar{R}_1 \sim Q\{1 \pm [1 + W/2Q^2]\} = -W/2Q \quad \text{(A20)}$$

and substitution from eq A4a yields

$$\bar{R}_1 \sim (k_{1A}k_{1B} - k_A k_B)/(k_{1A} + k_{1B}) \sim (k_{1A}k_{1B} - k_A k_B)/k_{1B} \quad \text{(A21)}$$

since $k_A \sim k_B$ and $R_{1B} \gg R_{1A}$, and therefore $k_{1B} \gg k_{1A}$. One immediately obtains from the above

$$\bar{R}_1 \sim k_{1A} - k_A k_B/k_{1B} \quad \text{(A22)}$$

Some algebraic manipulation and substitutions from eq A8 and A11 yield

$$\bar{R}_1 = R_{1A} + (k_A/k_B)R_{1B}k_B/(k_B + R_{1B}) = R_{1A} + ([ML]/[L])R_{1B}k_B/(k_B + R_{1B}) \quad \text{(A23)}$$

It is noteworthy that this final expression for the observed relaxation rate obtained in eq A23 is identical with that in eq A6 previously developed for the case of dilute paramagnetic species. No such restriction has been used in the present derivation. The only approximations applied here have been

(1) $k_{1A} \sim k_A$, since $k_A \gg R_{1A}$

$$(2)\ k_A \sim k_B \gg R_{1B}$$

$$(3)\ R_{1B} \gg R_{1A}$$

These approximations are based on typical experimental values for weak complexes of the lanthanides (except Gd) and ultimately lead to the truncation of the power series in eq A19 after the second term. The lead error, ϵ, of this approximation is, therefore, $\epsilon = (Q/8)x^2$, and it can be shown that the magnitude of the normalized lead error of the approximation is given by

$$|\epsilon|/\bar{R}_1 = \bar{R}_1/(k_A + k_{1B}) \sim \bar{R}_1/k_A \ll 1 \quad \text{(A24)}$$

In summary, we have shown that a simple expression, identical with that of dilute paramagnetic cases, can be derived for most systems of weak lanthanide complexes. This expression may be also applicable for other, non-lanthanide, systems in fast chemical exchange, provided that the same simple approximations about exchange rates and intrinsic relaxation rates are valid.

In the present system of dysprosium and glycocholate, one can easily show that since δ_M(Gly-α) = 28 ppm (Mukidjam et al., 1986) and conditions of fast exchange do prevail, the lower limit for k_B is of the order of 10^5 s^{-1}. Since $K_d \sim 10^{-3}$ M and [M] $\sim 10^{-3}$ M, according to eq A9, A10, and A12, $k_A \sim k_B > 10^5$ s^{-1}. The largest R_{1B} is $\sim 8 \times 10^2$ s^{-1}, and therefore, all necessary approximations are valid.

Registry No. Sodium glycocholate, 16409-34-0; calcium glycocholate, 77027-91-9.

References

Barnes, S., & Spenney, J. G. (1980) *Clin. Chim. Acta 102*, 241–245.

Barnes, S., & Geckle, J. M. (1982) *J. Lipid Res. 23*, 161–170.

Bevan, G., Engert, R., Klipstein, F. A., Maldonaldo, N., Rubulis, A., & Turner, M. D. (1974) *Gut 15*, 254–259.

Bloembergen, N., & Morgan, L. O. (1961) *J. Chem. Phys. 34*, 842.

Burns, P. D., & La Mar, G. N. (1982) *J. Magn. Reson. 46*, 61–68.

Carey, M. C., & Small, D. M. (1978) *J. Clin. Invest. 61*, 998–1026.

Choppin, G. R. (1971) *Pure Appl. Chem. 27*, 23–41.

Darnall, D. W., & Birnbaum, E. R. (1970) *J. Biol. Chem. 245*, 6484–6488.

Einspahr, H., & Bugg, C. E. (1981) *Acta Crystallogr., Sect. B: Struct. Crystallogr. Cryst. Chem. B37*, 1044–1052.

Elgavish, G. A., & Barnes, S. (1983) *Hepatology (Baltimore) 3*, 864 (Abstr.).

Gueron, M. (1975) *J. Magn. Reson. 19*, 58–66.

Hogan, A., Ealick, S. E., Bugg, C. E., & Barnes, S. (1984) *J. Lipid Res. 25*, 791–798.

Horrocks, W. DeW., Jr., & Sudnick, D. R. (1979) *J. Am. Chem. Soc. 101*, 334–340.

IUPAC–IUB Commission on Biochemical Nomenclature (1970) *Biochemistry 9*, 3471–3479.

Kahn, M. J., Lakshminarayanajah, N., Trotman, B. W., Chun, P., Kaplan, S. A., & Margulis, C. (1982) *Hepatology (Baltimore) 2*, 732.

Kibe, A., Dudley, M. A., Halpern, Z., Lynn, M. P., Brewer, A. C., & Holzbach, R. T. (1985) *J. Lipid Res. 26*, 1102–1111.

Lee, L., & Sykes, B. D. (1980) *Biophys. J. 32*, 193–210.

Leigh, J. S. (1971) *J. Magn. Reson. 4*, 308–311.

Lenkinski, R. E. (1984) *Biol. Magn. Reson. 6*, 23–71.

Lenkinski, R. E., & Reuben, J. (1976) *J. Am. Chem. Soc. 98*, 4065–4068.

Lenkinski, R. E., Elgavish, G. A., & Reuben, J. (1978) *J. Magn. Reson. 32*, 367–376.

Luz, Z., & Meiboom, S. (1964) *J. Chem. Phys. 40*, 2686–2692.

Marteau, C., Portugal, H., Pauli, A.-M., & Gerolami, A. (1985) *Hepatology (Baltimore) 5*, 1209–1212.

Matthews, B. W., & Weaver, L. H. (1974) *Biochemistry 13*, 1719–1725.

McConnel, H. M. (1958) *J. Chem. Phys. 28*, 430–431.

Moore, E. (1984) *Hepatology (Baltimore) 4*, 228S–243S.

Moore, E., Celic, L., & Ostrow, J. D. (1982) *Gastroenterology 83*, 1079–1089.

Moore, E., Ostrow, J. D., & Hofmann, A. F. (1985) *Gastroenterology 88*, 1679.

Mukidjam, E., Barnes, S., & Elgavish, G. A. (1986) *J. Am. Chem. Soc. 108*, 7082–7089.

Nieboer, E. (1975) *Struct. Bonding (Berlin) 22*, 1.

O'Reilly, D. E., & Poole, C. P., Jr. (1963) *J. Phys. Chem. 67*, 1762.

Poole, C. P., Jr., & Farach, H. A. (1971) in *Relaxation in Magnetic Resonance*, p 228, Academic, New York.

Purdie, N., & Farrow, M. M. (1973a) *Coord. Chem. Rev. 11*, 189.

Purdie, N., & Farrow, M. M. (1973b) *J. Solution Chem. 2*, 513–524.

Rajagopalan & Lindenbaum, S. (1982) *Biochim. Biophys. Acta 711*, 66–74.

Reuben, J. (1979) in *Handbook on the Physics and Chemistry of Rare Earths* (Gshneider, K. A., Jr., & Eyring, L., Eds.) Vol. 4, Chapter 39, pp 515–552, North-Holland, Amsterdam.

Reuben, J., & Elgavish, G. A. (1979) in *Handbook on the Physics and Chemistry of Rare Earths* (Gshneider, K. A., Jr., & Eyring, L., Eds.) Vol. 4, Chapter 38, pp 483–514, North-Holland, Amsterdam.

Roda, A., Hofmann, A. F., & Mysels, K. J. (1983) *J. Biol. Chem. 258*, 6362–6370.

Small, D. M. (1971) in *The Bile Acids* (Nair, P. P., & Kritchevsky, D., Eds.) pp 249–356, Plenum, New York.

Solomon, I. (1955) *Phys. Rev. 99*, 559.

Sowadski, J., Cornick, G., & Kretsinger, R. H. (1978) *J. Mol. Biol. 124*, 123–132.

Vega, A. J., & Fiat, D. (1976) *Mol. Phys. 11*, 347–355.

Westergaard, H. (1977) *Scand. J. Gastroenterol. 12*, 115–122.

Wheeler, H. O. (1968) in *Handbook of Physiology* (Code, C. F., Ed.) Section 6, pp 2403–2431, American Physiological Society, Washington, DC.

Williamson, B. W. A., & Percy-Robb, I. W. (1979) *Biochem. J. 181*, 61–66.

Williamson, B. W. A., & Percy-Robb, I. W. (1980) *Gastroenterology 78*, 696–702.